Available online at www.sciencedirect.com
SCIENCE DIRECT®
ELSEVIER
Earth and Planetary Science Letters 219 (2004) 325–340
EPSL
www.elsevier.com/locate/epsl

Changes in the carbon cycle during the last deglaciation as indicated by the comparison of ^{10}Be and ^{14}C records

Raimund Muscheler [a,*], Jürg Beer [b,**], Gerhard Wagner [b], Carlo Laj [c], Catherine Kissel [c], Grant M. Raisbeck [d], Françoise Yiou [d], Peter W. Kubik [e]

[a] GeoBiosphere Science Centre, Department of Geology, Quaternary Sciences, Lund University, Sölvegatan 12, SE-22362 Lund, Sweden
[b] Swiss Federal Institute of Environmental Science and Technology (EAWAG), CH-8600 Dübendorf, Switzerland
[c] Laboratoire des Sciences du Climat et de l'Environnement (CEA-CNRS), 91198 Gif-sur-Yvette, France
[d] Centre de Spectrométrie Nucléaire et de Spectrométrie de Masse, Centre National de la Recherche Scientifique, 91405 Orsay-Campus, France
[e] Paul Scherrer Institute of Particle Physics, HPK H30, ETH Hoenggerberg, CH-8093 Zürich, Switzerland

Received 20 June 2003; received in revised form 17 November 2003; accepted 8 December 2003

Abstract

The variations in atmospheric radiocarbon (^{14}C) concentration during the last 50 000 years can be attributed to changes in the ^{14}C production rate (due to changes in solar activity, the geomagnetic field and/or interstellar galactic cosmic ray flux) and to changes in the global carbon cycle. The relative contributions of these processes is the subject of current debate. Although the discrepancies between the various reconstructions of the past atmospheric radiocarbon concentration increase with age, the relatively good agreement over the last 25 000 years allows a quantitative discussion of the causes of the observed ^{14}C variations for this period. Using ^{10}Be measurements from Greenland Summit ice cores, we show that, in addition to solar and geomagnetically induced production rate changes, significant changes in the carbon cycle have to be considered to explain the measured ^{14}C concentrations. There is evidence that these changes are connected to: (1) global deglaciation and (2) climate changes in the North Atlantic region on centennial to millennial time scales related to changes in the ocean circulation. Differences between ^{10}Be and geomagnetic field records, however, suggest that uncertainties of about 20% still exist in determinations of past changes in the ^{14}C production rate.

Keywords: cosmogenic radionuclides; ice cores; carbon cycle; ocean circulation; paleomagnetism

1. Introduction

The cosmogenic radionuclide ^{14}C is produced in the Earth's atmosphere mainly by the interaction of cosmic rays with nitrogen [1]. Since the galactic cosmic ray flux is modulated by geo- and heliomagnetic shielding [1,2], records of ^{14}C and other cosmogenic radionuclides provide in-

* Corresponding author. Fax: +46-46-222-4830.
** Corresponding author. Fax: +41-1-823-5210.
E-mail addresses: raimund.muscheler@geol.lu.se (R. Muscheler), beer@eawag.ch (J. Beer).

0012-821X/04/$ – see front matter © 2004 Elsevier B.V. All rights reserved.
doi:10.1016/S0012-821X(03)00722-2

formation on variations in the solar activity and the geomagnetic field intensity in the past. After oxidation to $^{14}CO_2$, radiocarbon becomes a constituent of the global carbon cycle and exchanges between atmosphere, biosphere and the ocean. The ocean, as the largest reservoir of the ^{14}C cycle, plays the most important role in this system: variations in oceanic ^{14}C uptake influence the atmospheric radiocarbon concentration, since the oceanic residence time of ^{14}C is of the same order of magnitude as the ^{14}C half-life of 5730 years [3]. The analysis of past atmospheric ^{14}C concentration therefore provides the possibility to detect changes in the carbon cycle connected with changes in oceanic ventilation. This is of particular interest in connection with the large climatic changes during the transition from the last ice age to the Holocene [4]. However, since the atmospheric ^{14}C concentration is very sensitive to changes in the ^{14}C production rate [3], an accurate independent reconstruction of the past ^{14}C production rate is a prerequisite for a quantitative analysis of past variations in the carbon cycle based on ^{14}C. The idea of this paper is to estimate the past ^{14}C production rate changes based on the ^{10}Be records from Summit in central Greenland. We show that climatic changes connected to the deglaciation influence the ^{10}Be flux to Summit in the order of 20% or less. The ^{10}Be-based estimate for the ^{14}C production implies strong changes in the carbon cycle to explain the atmospheric ^{14}C concentration. Since there are differences to geomagnetic field-based ^{14}C production rates we present an alternative explanation based on a 'climate-corrected' ^{10}Be flux that implies a smaller influence of long-term changes in the carbon cycle on atmospheric ^{14}C concentration.

In a recent paper [5] some of the present authors simulated past changes of atmospheric ^{14}C concentration based on: (i) a geomagnetic intensity record retrieved from oceanic sediments and (ii) a new record of changes in the strength of the North Atlantic Deep Water (NADW) formation. These data are detailed for marine isotope stages (MIS) 2 and 3 (about half-millennial resolution) but their resolution is lower over the last 20 000 years. In particular the NADW record is very schematic for this last period. In this paper, we address the issue of past changes of atmospheric ^{14}C concentration using a different approach. Taking advantage of the fact that ^{14}C and ^{10}Be are produced by similar processes in the atmosphere [1,2] but have a completely different geochemical behavior, we use a new, high-resolution ^{10}Be record from the GRIP and GISP2 ice cores from Summit to estimate past variations in ^{10}Be and ^{14}C production rates. After its production, ^{10}Be becomes attached to aerosols and is removed from the atmosphere after a mean residence time of 1–2 years [6]. Therefore, provided that atmospheric processes affecting ^{10}Be are understood, ^{10}Be records from ice cores provide rather direct estimates of the variable production rate of the cosmogenic radionuclides. Such a comparison of ^{14}C production rate reconstructions based on ^{10}Be with measured ^{14}C data [7,8] has the potential to take into account all probable causes of production rate variations such as variations in geomagnetic field, solar activity and/or in the interstellar galactic cosmic rays flux. He we use this comparison to model changes in the global carbon cycle over the past 25 000 years.

2. The ^{10}Be record from the GRIP and GISP2 ice cores

At the moment, neither a ^{10}Be nor a ^{36}Cl (which is produced similarly as ^{10}Be) record exists that covers the 0–50 000 year interval without interruption. However, it is possible to construct a composite spliced ^{10}Be record by combining data from the GRIP and GISP2 ice cores that were recovered at Summit in central Greenland from locations approximately 30 km apart (Appendix and Fig. 1). A relationship between climate variations, illustrated by the climate proxy $\delta^{18}O$ measured in the GRIP ice core (Fig. 1c), and the ^{10}Be concentration is visible: during cold periods, which correspond to low $\delta^{18}O$ values, the ^{10}Be concentration is generally increased. This correlation is mainly due to a variable accumulation rate [9,10]. To remove this climatic component we have calculated the ^{10}Be flux, using the accumulation rate based on a semi-empirical relationship

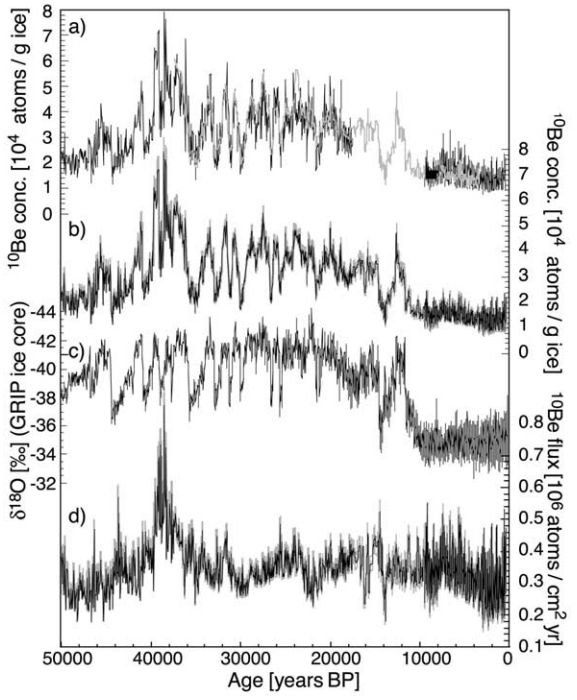

Fig. 1. ^{10}Be concentration and ^{10}Be flux measured in the Summit ice cores together with the climate proxy δ^{18}O. (a) ^{10}Be data from the GRIP ice core (black line) [9,17] including more than 1500 previously unpublished ^{10}Be measurements. The GISP2 data cover the time ranges of approximately 3300–8000 yr BP and 9300–37 500 yr BP (gray line) [15]. (b) Composite ^{10}Be concentration record. (c) GRIP δ^{18}O data [31] (note that δ^{18}O is plotted inversely). (d) Composite ^{10}Be flux record. Systematic errors due to differences between the different methods of combining the data are shown in gray in panels b and d. Differences between corresponding ^{10}Be measurements of the GRIP and GISP2 cores are in the order of 10%. These errors are not shown since they are only of minor importance for the following calculations. The curves are plotted versus the GRIP time scale [49].

between ice flow-corrected annual layer thicknesses and corresponding δ^{18}O values of the GRIP ice core back to 14 500 yr BP which was extrapolated further back in time [11]. These accumulation rates differ by up to 50% [10] from the published data for the GISP2 ice core which are obtained from layer counting and ice flow modelling for the complete last 50 000 years [12]. Support for using the published accumulation rate for the GRIP ice core comes from new data from the NorthGRIP (NGRIP) ice core. Due to the ice flow and melt characteristics at NGRIP the annual layers are much thicker in the lower part of the core and it is much less problematic to count the annual layers. These data confirm to a large extent the published accumulation rate from the GRIP ice core. In particular the expected strong dependence between past accumulation rates and isotopes, as assumed for the GRIP accumulation rate, is confirmed (Sigfus Johnsen, personal communication). This important correlation is, however, not always so obvious in the GISP2 accumulation rate record prior to the Bølling period.

Fig. 1d shows the ^{10}Be flux obtained from the spliced GRIP and GISP2 ^{10}Be concentration record. In contrast to the ^{10}Be concentration, the ^{10}Be flux is not influenced by the large climatic fluctuations during the last ice age. Linear regression analysis shows that the shared variance of the ^{10}Be flux and δ^{18}O is smaller than 6% for the last 50 000 years. Variations in atmospheric transport or incomplete atmospheric mixing of ^{10}Be could perturb a direct relationship between global ^{10}Be production and the ^{10}Be flux to Summit. In the case of the Summit ice cores, however, the good agreement of independent geomagnetic field reconstructions with the Summit radionuclide data suggests that, at least for MIS 3 ($\sim$20 000–60 000 yr BP), the ^{10}Be flux at Summit is determined mainly by production rate variations due to geomagnetic field intensity variations [13,14]. In addition, the good correlation between ^{10}Be and ^{14}C records during the Holocene [15,16] and the discovery of solar cycles in the ^{10}Be flux to Summit for the last ice age [17] are indications that the ^{10}Be deposition at Summit reflects the global ^{10}Be production rate variations caused by solar variability. Based on these earlier results we assume a linear relationship between the ^{10}Be flux to Summit and the global ^{10}Be production rate. This assumption allows us to calculate the past ^{14}C production rate based on the ^{10}Be flux and will be critically reviewed in Section 6.

3. Radiocarbon data

Reconstructions of past atmospheric radiocarbon concentrations are usually presented in terms

of $\Delta^{14}C$ defined as the per mil deviation from the National Institute of Standards and Technology ^{14}C standard after correction for decay and fractionation [18]. For the Holocene period the data shown in Fig. 2b are obtained from tree ring measurements [19]. For the pre-Holocene period the various $\Delta^{14}C$ data sets from several natural archives are based on different methods to infer independent time scales, which are crucial to determine $\Delta^{14}C$ [18]. They are based on varve chronologies [20–22], U/Th-dated corals, speleothems and sediments [23–26], and on correlations between oxygen isotope records of marine sediments and ice cores [27]. The high precision data from tree rings [19] show a moderate long-term decrease of the order of 100‰ during the Holocene. The increasing discrepancies between the different data sets for the pre-Holocene period indicate that there are unresolved problems in at least some of the data sets. One important source of uncertainty lies in the difficulty to accurately date the ^{14}C samples. Even a small dating error of 80 years results in a $\Delta^{14}C$ error of 10‰. In spite of the considerable scatter between the different reconstructions, the $\Delta^{14}C$ data consistently show fairly high values in the order of 400–600‰ for the period from 25 000 to 20 000 yr BP and a subsequent large decrease to approximately 100‰ at 10 000 yr BP. Prior to 25 000 yr BP the inconsistencies among the different $\Delta^{14}C$ data sets become very large. The thick gray curve in Fig. 2b shows a reconstruction of an average $\Delta^{14}C$ for the last 25 000 years. This curve is based on only tree ring measurements for the Holocene and on all the presented data for the pre-Holocene period after applying a 20-point running average. This curve basically agrees with the INTCAL98 calibration curve [19] except for two main differences. First, around 13 000 yr BP there is a difference mainly because we used the new high-resolution data from the Cariaco basin [21] plotted on the GRIP time scale and, in contrast to INTCAL98, we used all available $\Delta^{14}C$ data. Second, the INTCAL98 calibration curve shows a linear trend from 24 000 to 15 500 yr BP. The trend of our composite $\Delta^{14}C$ curve agrees basically with the INTCAL98 curve but it also shows shorter-term changes (see Fig. 2).

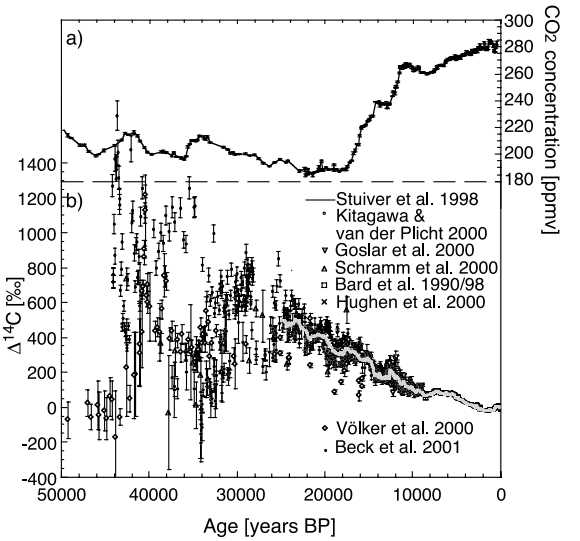

Fig. 2. Carbon dioxide and radiocarbon data for the last 50 000 years. (a) Different CO_2 measurements in Antarctic ice cores [28,34,52]. For the last deglaciation we only used the latest CO_2 data from Dome C ice core since it is possible to synchronize these data with the GRIP chronology via common CH_4 variability as proposed by Monnin et al. [34]. (b) Different reconstructions of the atmospheric radiocarbon concentration for the last 50 000 years. For the Holocene period, where $\Delta^{14}C$ is very well determined, only the tree ring measurements [19] are plotted. For the pre-Holocene period $\Delta^{14}C$ measurements in varved lake sediments [20,22,26,53], speleothems [23], corals [24,25], and sea sediments [21,27] are shown. The $\Delta^{14}C$ data from the Cariaco basin were synchronized to the GRIP time scale [16,21]. The uncertainties increase with age. The gray curve shows an average $\Delta^{14}C$ reconstruction (see text) for the last 25 000 years.

The relatively high $\Delta^{14}C$ values prior to and during the deglaciation can be explained by an increased ^{14}C production rate and/or reduced ^{14}C uptake by the oceans [3]. Reconstructions of the atmospheric CO_2 concentration (Fig. 2a), which, during the last ice age, only amounted to approximately two thirds of the Holocene mean value [28], point to substantial changes in the carbon cycle with a potentially important influence on $\Delta^{14}C$. The following discussion concentrates on the period from 25 000 to 10 000 yr BP, where the reasonable agreement between the various $\Delta^{14}C$ records allows us to estimate changes in the global carbon cycle from the $^{14}C/^{10}Be$ comparison.

4. $\Delta^{14}C$ variations inferred from the ^{10}Be-based production rate alone

We use the outcrop-diffusion model of Siegenthaler [29] (Appendix) to quantify the effects of the global carbon cycle on $\Delta^{14}C$. The first step was to hold the carbon cycle constant in order to determine to what extent the $\Delta^{14}C$ variations are caused by variations in the ^{14}C production rate alone. The result is shown in Fig. 3. The ^{10}Be-based and measured $\Delta^{14}C$ agree within the estimated errors during the Holocene even though the model overestimates the $\Delta^{14}C$ changes. Between 25 000 and 10 000 yr BP the two records show significant differences. The ^{10}Be-based $\Delta^{14}C$ exhibits almost no long-term trend, while the measured $\Delta^{14}C$ decreases from approximately 500 to 100‰. The ^{10}Be maximum around 40 000 yr BP leads to a $\Delta^{14}C$ increase of approximately 300‰ (see inset in Fig. 3). The $\Delta^{14}C$ band in Fig. 3 encompasses different simulations obtained from different ^{14}C production rate reconstructions arising from: (i) differences in the GRIP and GISP2 ^{10}Be data, (ii) different methods of normalizing and combining the data (Appendix), and (iii) differences in the calculation of the ^{14}C and ^{10}Be production rates [2,30]. It illustrates the uncertainties of our reconstruction of the ^{14}C production rate. Additional potential uncertainties due to errors in the accumulation rate or to changes in the ^{10}Be transport are difficult to assess and are not included. Even though the modelled $\Delta^{14}C$ band is large there are significant differences between ^{10}Be-based and measured $\Delta^{14}C$, especially prior to 15 000 yr BP.

5. Changes in ocean circulation as indicated by ^{10}Be and ^{14}C

The difference between measured and ^{10}Be-based $\Delta^{14}C$ suggests strong changes in: (i) the

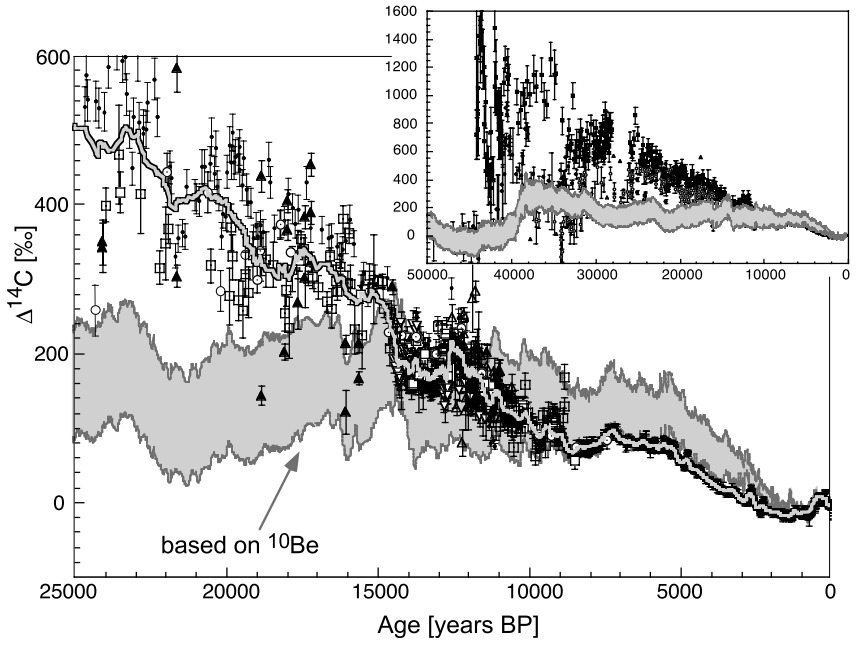

Fig. 3. Comparison of the measured $\Delta^{14}C$ with the ^{10}Be-based $\Delta^{14}C$ which was calculated under the assumption that no changes in the carbon cycle occurred during the last 50 000 years. The gray curve shows the combination of the different $\Delta^{14}C$ reconstructions (see Fig. 2). The ^{10}Be-based calculation (gray data) is shown with its error range (gray band). The uncertainty in modelled $\Delta^{14}C$ arises from the differences in the production rate calculations and in the ^{10}Be data from the GRIP and GISP2 ice cores. The modelled $\Delta^{14}C$ record is normalized to modern $\Delta^{14}C$ values (pre-bomb). The inset shows the comparison for the last 50 000 years.

global carbon cycle and/or (ii) the ^{10}Be transport to Summit during the deglaciation. Therefore, if we assume that the ^{10}Be flux to Summit is an accurate indicator of changes in global ^{10}Be production we have to include strong changes in the carbon cycle to explain the differences between ^{10}Be and Δ^{14}C.

The ocean is the largest radiocarbon reservoir, including more than 90% of the total ^{14}C inventory on Earth. Only processes involving the oceans have the potential to produce significant carbon cycle-related Δ^{14}C changes (e.g. [3]). In the following, we attribute the observed Δ^{14}C decrease from 20 000 to 10 000 yr BP to an increase in global oceanic ventilation, i.e. to an increase in the ^{14}C flux from the ocean surface to the deep ocean. However, it should also be kept in mind that other mechanisms, for instance a reduction in ^{14}C exchange rate between atmosphere and ocean due to changes in wind speed and/or sea ice cover, could also contribute to the observed Δ^{14}C changes [3].

Fig. 4 shows the difference between measured and ^{10}Be-based Δ^{14}C. The relatively small deviations during the Holocene indicate that no significant changes in ocean ventilation can be inferred during this period. Prior to 10 000 yr BP the difference between modelled and measured Δ^{14}C resembles the climate parameter δ^{18}O measured in the GRIP ice core [31]. The peaks of the Bølling/Allerød period, the minimum during the Younger Dryas as well as the long-term trend from 20 000 to 10 000 yr BP are visible in both the Δ^{14}C difference and the δ^{18}O record from Greenland. The long-term climate change is also visible in Antarctic ice cores (Fig. 4c) indicating a connection between global deglaciation and carbon cycle changes. The similarity between δ^{18}O from the GRIP ice core and the Δ^{14}C difference may imply that an increased deep-water formation in the North Atlantic was accompanied by a pronounced heat transport from lower latitudes to the north with corresponding changes in δ^{18}O [32]. It may corroborate the importance of the Atlantic meridional overturning circulation for the global ^{14}C distribution [33]. Fig. 4 also suggests a non-linear relationship between Δ^{14}C difference and δ^{18}O: climate changes on shorter time

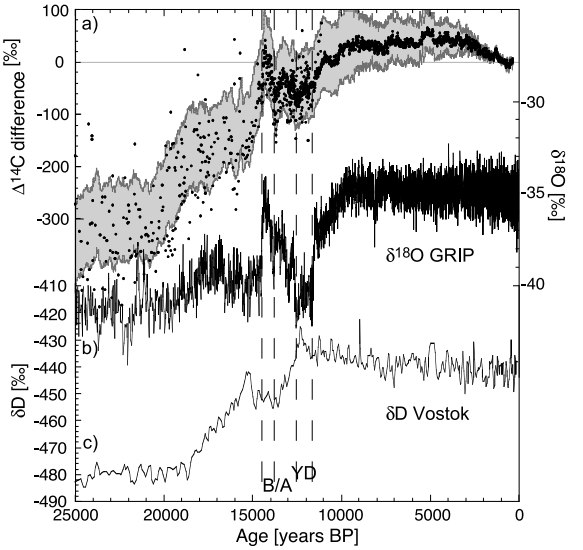

Fig. 4. Comparison of the differences between the ^{10}Be-based and measured Δ^{14}C with the climate proxies δ^{18}O and δD measured in polar ice cores. (a) The difference between the composite Δ^{14}C record and the different ^{10}Be-based Δ^{14}C model calculations (gray band). The points indicate the difference of the measured individual Δ^{14}C data to the mean ^{10}Be-based Δ^{14}C curve. (b) δ^{18}O record from the GRIP ice core [31]. (c) δD record from the Vostok ice core (East Antarctica) [54]. The data from Vostok are plotted on the GRIP time scale [55]. A/B and YD indicate Bølling/Allerød and Younger Dryas climate periods.

scales as, for example, those occurring during the Younger Dryas cause relatively weak differences of the order of 50 ‰ between measured and modelled Δ^{14}C. On the other hand the Δ^{14}C difference, which evolves from 20 000 to 10 000 yr BP, is in the order of 300 ‰.

It is interesting to note that reconstructions of the past atmospheric CO_2 concentration show fast step-like changes at the beginning of the Bølling/Allerød (around 14 500 yr BP) and the Holocene (11 550 yr BP) warm periods [34]. These changes occur synchronously with the changes in the Δ^{14}C difference shown in Fig. 4. It was suggested that these CO_2 changes could be connected to changes in the ocean thermohaline circulation [34], which is in agreement with our interpretation.

Fig. 5 shows the result of model runs taking into account variations in deep-water formation. For these calculations the oceanic ventilation was adjusted to obtain a match between the ^{10}Be-

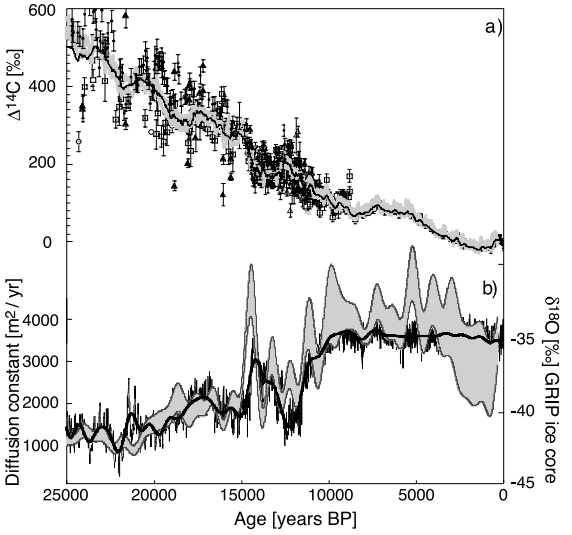

Fig. 5. Measured and modelled $\Delta^{14}C$ including changes in: (i) ^{14}C production and (ii) deep-water formation as indicated by the comparison of ^{10}Be and ^{14}C. The upper panel shows the measured $\Delta^{14}C$ data including the composite $\Delta^{14}C$ record (black curve) and the ^{10}Be-based $\Delta^{14}C$ curves (gray). The gray band in the lower panel shows the changes in ocean ventilation which have to be invoked to match ^{10}Be-based and measured $\Delta^{14}C$. The changes were low-pass filtered (cut-off frequency = 1/1000 yr^{-1}) to remove the short-term scatter. The gray bands show the uncertainties due to the differences in the reconstructions of the ^{14}C production rate. The dark gray line shows $\delta^{18}O$ measured in the GRIP ice core and the thin black line shows the low-pass filtered data (cutoff frequency = 1/1000 yr^{-1}).

based and the measured $\Delta^{14}C$. By permanently calculating the difference between reference value (measured $\Delta^{14}C$) and actual value (modelled) it is possible to adjust the diffusion constant in order to minimize this difference. If the modelled $\Delta^{14}C$ is too high this leads to a higher diffusion constant and vice versa. No trial-and-error approach is necessary for this calculation since this method allows us to reproduce the measured $\Delta^{14}C$ within each model run.

To explain the high $\Delta^{14}C$ values of approximately 400‰ for the period around 20 000 yr BP the ocean ventilation has to be reduced considerably. In our model a reduction of the diffusion constant to approximately 30% of the present value results in a good fit between ^{10}Be-based and measured $\Delta^{14}C$. A reduction of the diffusion constant in the order of 50% results in a good agreement for the period from 18 000 to 15 000 yr BP. The short-term variations in the $\Delta^{14}C$ difference from 15 000 to 10 000 yr BP (Fig. 4a) cause corresponding changes in the reconstructed ocean ventilation. During the Holocene the ocean ventilation changes are significantly less constrained. Changes in ventilation cause relatively small changes in $\Delta^{14}C$ during periods of generally increased ocean ventilation. This non-linear dependence of $\Delta^{14}C$ on circulation changes is the cause for the relatively large error band in Fig. 5 for the Holocene period. With the present data and knowledge of radionuclide systems, the relatively small differences between modelled and measured $\Delta^{14}C$ during the Holocene are within the uncertainty of our method.

In general, apart from the shorter-term fluctuations, a more or less linear increase in ocean ventilation can explain the measured $\Delta^{14}C$ decrease from 18 000 to 10 000 yr BP. This change is synchronous with long-term changes in paleoclimate records during the last deglaciation, as for example the increase in atmospheric CO_2 (Fig. 2a). However, the indicated $\Delta^{14}C$ changes due to decreased ventilation are beyond the changes to be expected from the present state of knowledge of the carbon cycle. More sophisticated models predict $\Delta^{14}C$ variations in the order of 40‰ or less for a realistic weakening in the thermohaline circulation [35]. Therefore, ocean circulation is probably not exclusively the cause for the long-term $\Delta^{14}C$ decrease during the deglaciation. There could be other processes causing the $\Delta^{14}C$ variations. For example, a new study indicates that the effects of changes in gas exchange rate between atmosphere and ocean have been underestimated so far [36]. A decreased gas exchange rate between atmosphere and ocean also leads to less ^{14}C transport to the deep ocean and increases atmospheric ^{14}C concentration. Therefore, independent reconstructions of ocean circulation changes (e.g. [37]) cannot be used to rule out carbon cycle changes as indicated by the $^{10}Be/^{14}C$ comparison. Independent reconstructions of ocean circulation changes could help to disentangle the different processes affecting atmospheric ^{14}C. Wunsch [38] for example claims that the evidence for increased oceanic mixing during the last glacial is more convincing

than the evidence for the opposite. If true this could indicate that other processes as mentioned above dominated the long-term changes in atmospheric ^{14}C concentration during the last 25 000 years. Until now alternative methods to reconstruct the ^{14}C distribution in the oceans do not show a consistent picture (e.g. [38–40]) and seem not yet to be useful to disentangle the different processes affecting atmospheric ^{14}C concentration changes.

From 15 000 to 10 000 yr BP the differences between measured and modelled $\Delta^{14}C$ with constant ventilation are in the order of 50‰ (Fig. 4a). It is important to note that the relatively large error band during this period is caused by the differences of the various ^{10}Be-based ^{14}C production rate reconstructions. For example, one combination of the GRIP and GISP2 data can yield a modelled $\Delta^{14}C$ at the upper limit of the uncertainty band and another one at the lower limit. This means that each of the modelled $\Delta^{14}C$ curves shows similar changes but with a different offset. Therefore, the relative changes of the modelled $\Delta^{14}C$ on centennial to millennial time scales are less uncertain during this period. The uncertainties are mainly due to the errors of the individual ^{10}Be measurements. These errors, which can be assessed by a Monte Carlo approach, are in the order of ±5‰ [16]. Since these errors are small compared to the systematic errors we did not include them in the figures. The magnitude of the $\Delta^{14}C$ variations from 15 000 to 10 000 yr BP is in agreement with the results of more complex carbon cycle models [35]. Therefore, these variations can be attributed to variations in the NADW formation. We postulate that two qualitatively different mechanisms could be responsible for the carbon cycle changes influencing $\Delta^{14}C$. The first attributes the $\Delta^{14}C$ variations to changes in NADW formation. The second mechanism for $\Delta^{14}C$ changes is associated with the long-term changes during the global deglaciation when the atmospheric CO_2 concentration, sea level, sea ice cover and global temperature changed significantly.

Also during the geomagnetic minimum around 40 000 yr BP we get a better correspondence between measured and modelled $\Delta^{14}C$ if we include changes in the carbon cycle. Although it is not possible to identify this geomagnetically induced $\Delta^{14}C$ increase unequivocally in all $\Delta^{14}C$ data sets, the peak of about 600‰ around 41 000 yr BP in the data from the North Atlantic has been first attributed to this event [41]. Other high values from stalagmite data have been reported by Beck et al. [23] but they are significantly older (44 000 yr BP). The ^{10}Be-based $\Delta^{14}C$ increases only about 300‰ neglecting changes in the carbon cycle. A decrease in the diffusion constant to 30% of the present value leads to a ^{10}Be-based $\Delta^{14}C$ increase of about 500‰ around 40 000 yr BP, which is in better agreement with the data. However, a strongly decreased ventilation to a constant value throughout the complete period of increased ^{10}Be deposition is very unlikely because it covers Dansgaard/Oeschger events 9 and 10 [13] which are connected to a variable ocean circulation [5].

6. Discussion

The basic assumption on which our conclusions depend is that the ^{10}Be flux at Summit in Greenland is proportional to the global ^{10}Be production rate. Here we will discuss the pros and cons of this assumption.

6.1. Comparison with other ^{14}C production records

The recent evaluation of atmospheric $\Delta^{14}C$ variations during MIS 2 and 3 [5], largely based on the NAPIS-75 paleomagnetic reconstruction, suggests that the high atmospheric radiocarbon concentration during the last glacial period is mainly (but not completely) due to low geomagnetic field intensities relative to the present value [5]. The difference with respect to the ^{10}Be-based $\Delta^{14}C$ mainly arises from the fact that the geomagnetic field-based and the ^{10}Be-based ^{14}C production rates differ by an average offset of approximately 20% before 18 000 yr BP. Fig. 6 shows the comparison of the ^{14}C production rates derived from the Summit ^{10}Be records and the most recent geomagnetic field compilation of Laj et al. [5] based on NAPIS-75. The comparison shows a very good

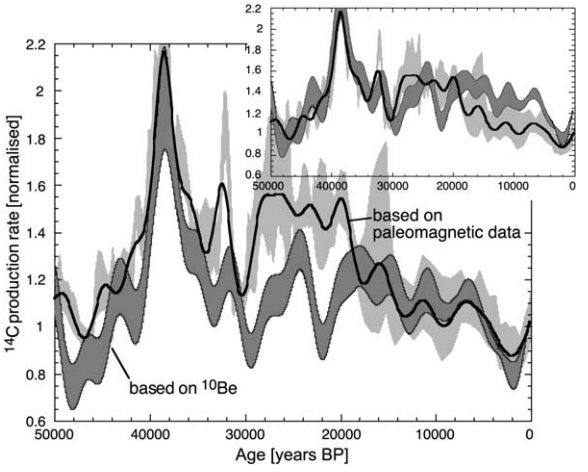

Fig. 6. Comparison of different reconstructions of the ^{14}C production rate for the last 50 000 years. The dark gray band shows the range of ^{10}Be-based ^{14}C production rates after low-pass filtering the data (cutoff frequency = 1/3000 yr^{-1}). The black line shows the ^{14}C production rates based on the paleomagnetic data [5] after applying the same low-pass filter. The light gray band shows the error range of the original data. The different records are shown on the GRIP time scale. The inset shows the same comparison after shifting the ^{10}Be-based ^{14}C production rate by +20%. After this modification the two independent ^{14}C production rates agree within the errors from 50 000 to 18 000 yr BP.

agreement for the last 18 000 yr BP and significant differences prior to 18 000 yr BP where the paleomagnetic field-based production rate suggests an increased ^{14}C production rate. As a consequence, neglecting changes in the carbon cycle, the geomagnetic field-based Δ^{14}C during the last ice age is higher compared to the ^{10}Be-based Δ^{14}C and results in a smaller difference between modelled and measured Δ^{14}C [5]. The differences between 60 000 and 18 000 yr BP could be caused by unresolved problems in the ^{10}Be or the geomagnetic field-based ^{14}C production rate. As mentioned uncertainties in the ^{10}Be-based ^{14}C production rate could be due to the reconstructed accumulation rate and possible deviations of the ^{10}Be flux from being proportional to the global ^{10}Be production rate throughout the last 50 000 years. However, the small differences between ^{10}Be-based and geomagnetic field-based ^{14}C production rate observed during the last 18 000 years are within the error limits (Fig. 6). If climate changes influenced the ^{10}Be transport to Summit we would expect to find the main disagreement during this period when the strongest climatic changes took place. In addition, if ^{10}Be is normalized differently the changes in geomagnetic field and radionuclide flux agree within the errors for the period from 60 000 to 20 000 yr BP [14,42] (Fig. 6, inset). If the differences in the order of 20% are caused by changes in the ^{10}Be system, this would indicate a relatively abrupt change in the ^{10}Be transport or deposition between 20 000 and 18 000 yr BP, which we cannot exclude. But also the geomagnetic field-based ^{14}C production rate has its uncertainties. The geomagnetic field reconstructions do not show solar activity changes which clearly are present in the time interval of interest [17]. If the disagreement shown in Fig. 6 is due to changes in solar activity this would point to a generally increased solar activity before 18 000 yr BP. Long-term changes in the interstellar cosmic ray intensity would also lead to ^{14}C production rate changes which cannot be reconstructed by geomagnetic field measurements. The disagreement between ^{10}Be and geomagnetic field-based ^{14}C production could also be caused by uncertainties in the geomagnetic field reconstruction due, in particular, to the difficulties in the calibration of the sedimentary record on an absolute scale. For the most recent period (11 000 years), the record is based on archeomagnetic data. Although representing spot readings of the field, these data are numerous enough and widely distributed over the northern hemisphere, so that their average can be considered to be a relatively precise estimate of the dipole field. Beyond 12 000 years, less abundant volcanic data are available. Like many marine sedimentary records, NAPIS-75 does not extend into the last 15 000–20 000 years because the uppermost part of the cores is at best disturbed, sometimes missing and in most cases too soupy for reliable magnetic measurements to be done. Therefore, the overlap with sedimentary records which, in a good quality, extend only to about 15 000–18 000 yr BP, is thus limited, precluding an unambiguous, precise connection between relative (sedimentary) and absolute data. The long-term differences in the ^{10}Be and geomagnetic field-based Δ^{14}C record could be reconciled using a

normalization of the sedimentary record slightly different from that given in the previous evaluation [5]. This normalization, although in our opinion less realistic, would still be within error limits of the presently available data set. However, reconciling some of the short-term differences would still be problematic.

Other geomagnetic field reconstructions based on marine sediments [43] or marine ^{10}Be records [44] show a geomagnetic field minimum around 40 000 yr BP and a subsequent almost linear increase towards the Holocene. The minimum around 40 000 yr BP is in agreement with the Summit ^{10}Be record and the most recent geomagnetic field compilation of Laj et al. [5]. However, in contrast to the global geomagnetic field compilations by Guyodo and Valet [43] and the geomagnetic field reconstruction based on ^{10}Be measurements in sediments [44], the Summit ^{10}Be- and the NAPIS-75-based records [5] show a much more variable geomagnetic field history during the last 50 000 years. One main reason is that the time resolution of these global geomagnetic field compilations is very low. For example, the reconstruction by Guyodo and Valet [43] does not capture the fine structure during the Holocene which leads to disagreements with the estimate of global geomagnetic field changes based on archeomagnetic data [45]. The same applies for geomagnetic field reconstructions based on ^{10}Be measurements in sediments [44]. In addition, these records are strongly influenced by changes in the ^{10}Be transport to the sediment [46] making it difficult to extract the pure production signal [47]. Nevertheless, these records point to a generally increased ^{14}C production during the last ice age compared to the Summit ^{10}Be record and rather agree with the NAPIS-75-based record.

With our present knowledge of the radionuclide systems and the uncertainties of the paleomagnetic records, we cannot pinpoint the origin of the differences between the ^{10}Be- and geomagnetic field-based ^{14}C production rates (Fig. 6). In the following we will discuss some characteristics of the carbon cycle, which may help to distinguish between production and carbon cycle effects and their effect on the atmospheric ^{14}C concentration.

6.2. Characteristics of Δ^{14}C changes

Changes in the production rate and changes in the ocean ventilation influence Δ^{14}C with two widely different time constants. A step change in the production rate causes Δ^{14}C changes with a time constant of about 5000 years (Fig. 7a). This time constant is mainly determined by the half-life of ^{14}C. By contrast, changes in oceanic ventilation, which mean a redistribution of ^{14}C in the ocean, lead to much faster Δ^{14}C changes on time scales of centuries (Fig. 7b). This disparity of time scales has important implications for the comparison of ^{10}Be and ^{14}C at the transition from the ice age to the Holocene. It implies that

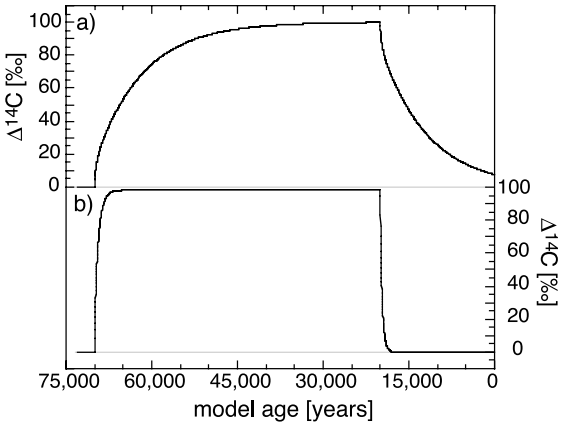

Fig. 7. Reaction of atmospheric ^{14}C concentration on stepped changes in the ^{14}C production rate and in the oceanic ventilation. (a) A model run where the ^{14}C production rate is increased by 10% at 70 000 years and reduced to the original value at 20 000 years. As expected, the atmospheric ^{14}C content rises by 10% in all reservoirs producing a corresponding Δ^{14}C increase of 100‰. It takes approximately 5000 years until the atmospheric ^{14}C content has increased by 5% after the ^{14}C production rate increase. After returning to the original ^{14}C production rate at 20 000 years the atmospheric ^{14}C content decays almost exponentially with a characteristic time of 5000 years. (b) A model run where the ocean mixing coefficient is reduced to 50% at 70 000 years and restored to its original value at 20 000 years. Half of the Δ^{14}C increase occurs during approximately 350 years after the circulation change and half of the decrease occurs already in less than 200 years. This change in the ocean mixing produces a comparable Δ^{14}C change as in the run shown in panel a. However, the time scales on which these changes occur are very different.

changes in ocean ventilation during the deglaciation can have only a short-lasting effect on $\Delta^{14}C$ restricted only to the beginning of the Holocene. On the contrary, any error in the calculated production rate, for example due to changes in ^{10}Be transport during deglaciation, would lead to errors in the modelled $\Delta^{14}C$ during the entire Holocene.

This long-term 'memory' of the ^{14}C system is illustrated in Fig. 8. It shows a calculation where we assigned the difference between modelled and measured $\Delta^{14}C$ during the deglaciation to changes in the ^{10}Be system. We introduced a 'correction factor' for the ^{10}Be flux of 1.2 for the period prior to 20 000 yr BP. The multiplicative factor linearly decreases to 1.0 from 20 000 to 18 000 yr BP (see Fig. 8a). This modification reconciles to a large extent the ^{10}Be- and geomagnetic field-based ^{14}C production rates. As expected the agreement of modelled and measured $\Delta^{14}C$ for the pre-Holocene period improves considerably when this modification is considered, but, because of the memory effect, we obtain a worse fit for the Holocene. Compared to the tree ring data the modelled $\Delta^{14}C$ based on the modified ^{14}C production rate is approximately 80‰ too high at the beginning of the Holocene which is, in contrast to the unmodified ^{10}Be-based curve, not within the estimated errors. Since the unmodified ^{10}Be-based $\Delta^{14}C$ already rather overestimates the Holocene $\Delta^{14}C$ changes this modification leads in the wrong direction if we would concentrate only on the Holocene period. Therefore, if this modification is correct this would imply additional changes in the carbon cycle during the Holocene that are similar or even stronger than during the glacial. This, however, seems to be rather improbable. Therefore, if we have to include a correction in the ^{10}Be flux to obtain the global mean ^{10}Be production rate we have also to imply such changes during the relatively stable Holocene period.

However, one should be aware that the modelled $\Delta^{14}C$ is very sensitive to small changes in the ^{14}C production rate. Differences in the order of 20% produce $\Delta^{14}C$ differences of 200‰ in the long term. Beside the 20% difference prior to 20 000 yr BP, the overall agreement between geomagnetic field and ^{10}Be flux is very good. The 20% difference is almost within the estimated errors of our methods but it has, as we showed in this paper, important consequences for the inferred origins of the $\Delta^{14}C$ changes.

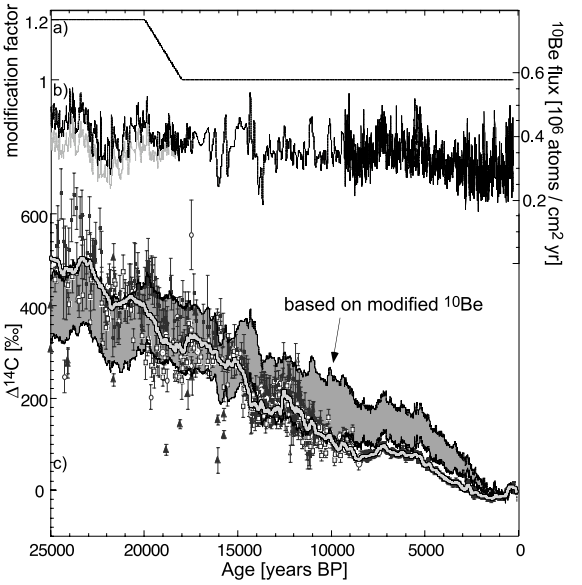

Fig. 8. Comparison of measured $\Delta^{14}C$ with ^{10}Be-based $\Delta^{14}C$ after the modification of the ^{10}Be fluxes and ^{14}C production rates. (a) Adjustment function used to modify the ^{10}Be flux. (b) Modified ^{10}Be fluxes. (c) Comparison of measured $\Delta^{14}C$ and modelled $\Delta^{14}C$ based on modified ^{10}Be flux. The band in panel c indicates the uncertainties due to the differences in the reconstruction of the ^{14}C production rate.

Additional measurements of continuous ^{10}Be records from other ice cores in particular from Antarctica and their comparison with the Summit ^{10}Be record could improve the accuracy of our reconstruction of the ^{14}C production rate. The measurement of continuous ^{36}Cl time series could further improve the situation, since ^{10}Be and ^{36}Cl are produced similarly but behave differently in the atmosphere.

7. Conclusions

The comparison of ^{10}Be and ^{14}C gives insight into the factors responsible for atmospheric ^{14}C concentration changes over the last 25 000 years.

We obtain a high degree of similarity between ^{10}Be-based and measured Δ^{14}C for the last 10 000 years pointing to a dominant influence of common variations in the production rate. Prior to 10 000 yr BP there are clear differences between measured and modelled Δ^{14}C which can be attributed to variations in the carbon cycle and/or to variations in the ^{10}Be system. Assuming that the ^{10}Be flux to Summit is mainly influenced by the variable production this comparison points to considerable changes in the carbon cycle during the last deglaciation resulting in a generally decreased oceanic ^{14}C uptake during the last ice age. The inferred variations in the carbon cycle show a close connection to δ^{18}O measured in the Greenland ice cores on centennial to millennial time scales and on the time scale of the deglaciation. Due to differences between geomagnetic field- and ^{10}Be-based ^{14}C production rates and due to the required accuracy our conclusions on the long-term carbon cycle changes are more uncertain than on the changes on millennial time scales. Assuming a change in atmospheric ^{10}Be transport in the order of 20% before 18 000 yr BP reconciles the Summit ^{10}Be record and independent geomagnetic field reconstructions. This comparison suggests that the long-term changes in the carbon cycle could be overestimated by the comparison of Summit ^{10}Be record and Δ^{14}C. For the period prior to 25 000 yr BP, no final answer can be given as long as the problem of the scatter between the various Δ^{14}C reconstructions is not resolved. Common variability in ^{10}Be and Δ^{14}C records, as for example the Δ^{14}C decrease from 23 000 to 21 500 yr BP (see Figs. 3 and 8), could help to improve the Δ^{14}C time scales which are one important source of uncertainty in the Δ^{14}C data.

Acknowledgements

We would like to thank Alain Mazaud, Claire Wedema, David Livingstone, Olivier Marchal, and five anonymous reviewers for helpful discussions and comments on the manuscript. This work was supported by the Swiss National Science Foundation.*[BARD]*

Appendix A

A.1. The spliced ^{10}Be record

The GRIP ^{10}Be concentration measurements cover the Holocene period from 300 to 9300 yr BP (non-continuously but without gaps longer than 30 years) and the last ice age until 17 400 yr BP (with fewer gaps). The time resolution of the data shown in Fig. 1 ranges from 2 to 3 years in the youngest part of the ice core up to ~40 years at 50 000 yr BP [9,17]. More than 1500 previously unpublished ^{10}Be measurements [48] mainly fill the gaps in the Holocene part of the record [9] and smaller gaps in the glacial part. The GISP2 data [15] cover the time intervals 3300–7850 and 9300–37 500 yr BP. The time resolution of GISP2 ^{10}Be data is approximately six times lower than for the GRIP data. The GISP2 data were transferred to the GRIP time scale by synchronizing the δ^{18}O data sets of the GRIP [49] and GISP2 [50] ice cores and the data are reported on the GRIP time scale [49]. For the intervals where the two records overlap a comparison of the ^{10}Be concentrations reveals that the two data sets are strongly correlated. Linear regression analysis indicates a shared variance of 92% ($n = 256$). Furthermore, after normalization of the GISP2 data to the beryllium standard which was used for the GRIP measurements (SRM 4325 [9]) the mean values of the data differ by less than 3%. However, when investigating special time periods differences up to 10% are visible. For the Holocene period when the two records overlap the GISP2 data are in the mean approximately 7% lower than the GRIP data. For the period 17 000–37 500 yr BP the GISP2 data are approximately 6% higher than the GRIP values. Because of these differences we estimate that potential errors in the ^{10}Be data are in the order of 10%. These differences could be due to incomplete age coverage due to still lacking data (by e.g. coincidentally missing some solar maxima in one data set) and the possible differences in the transport and/or deposition of ^{10}Be at the two sites. Furthermore, the different methods of sample preparation and separating the dust from the ice [9,15,51] might cause differences in the order of

10% for the period of the last ice age. For example we corrected GRIP samples which were processed with the 0.45 μm filters by adding 25% to correct for the ^{10}Be removed by the filter [9,51] while the GISP2 data were corrected by measuring all filters and by summing the filter-borne and filtrate ^{10}Be [15]. Surprisingly the dust-borne fraction of ^{10}Be seems not to be related to the changes in climate [51] which allows this general correction for the last ice age. These methods were applied for each sample older than 11 500 years. Nevertheless, taking into account these uncertainties the combined data set can be considered to be representative of the ^{10}Be concentration at Summit. To calculate the spliced ^{10}Be record shown in Fig. 1b we have applied different methods to correct for the systematic differences in the ^{10}Be concentration described above. For periods with overlapping data we have interpolated the GISP2 ^{10}Be data to the GRIP time resolution. To assess the uncertainties due to the differences in the ^{10}Be data, we calculated several spliced ^{10}Be records with different normalizations of the GISP2 and GRIP ^{10}Be data. For example, one record was obtained after correcting for the systematic difference during the Holocene (all GISP2 data +7%) and another record after correction for the systematic difference during the last ice age (all GISP2 data −6%). These curves were included in the calculations of Δ^{14}C and can be considered a good measure for the systematic uncertainties of the data. Differences between the individual data points are bigger (the average 1σ errors for the means between GRIP and GISP2 ^{10}Be data values are 10%).

A.2. Reconstruction of the ^{14}C production rate

To calculate the ^{14}C production rate variations from the ^{10}Be flux we assume that long-term (>3000 years) variations are due to the varying geomagnetic field [14]. We attribute the variations occurring on shorter time scales to changes in solar activity. This separation is applied because geomagnetic field and solar activity variations influence the ^{14}C and ^{10}Be production rates in a slightly different way [2,30]. However, since these differences between solar- and geomagnetic field-induced production changes are relatively small, our results do not depend strongly on the assumption necessary to convert the ^{10}Be flux to the ^{14}C production rate. Potential variations in the interstellar cosmic ray flux are not explicitly considered in this calculation but they should show up in the ^{10}Be flux and therefore also in the reconstructed ^{14}C production rate. We used both the results of the production calculations of Masarik and Beer [2] and Lal [30] to reconstruct the ^{14}C production rate. Together with the different combinations of the ^{10}Be data we obtained 14 different reconstructions of the ^{14}C production rate which were the basis to draw the error bands shown in the figures.

A.3. Carbon cycle model

There is a variety of different carbon cycle models but at least on longer time scales the choice of the model does not influence the results (assuming constant carbon cycle). For example a 10% increase in the ^{14}C production rate leads to a 10% increase of the ^{14}C content in every carbon reservoir for steady-state conditions. Therefore, including a constant sink in the model, as for example an ocean sediment box, does not change the results on long time scales. However, changes in the exchange fluxes or in the corresponding sizes of the ^{14}C reservoirs can have a significant influence on Δ^{14}C, if such changes are included during a model run. We use the outcrop-diffusion ocean model of Siegenthaler [29] to calculate Δ^{14}C using the ^{10}Be-based ^{14}C production rates. This model includes atmosphere, biosphere and ocean. We used the set-up where the mixing of carbon within the ocean is described only by diffusive exchange ($a_c = 0$, $F_{as} = 17.99$ mol m^{-2} yr^{-1}, $K = 4005$ m^2 yr^{-1}, see [29]). A reduced oceanic deep water formation is then described by a reduced diffusion constant. Differences to other carbon cycle models, as for example used in Laj et al. [5], are small. The effect of the variation in atmospheric CO_2 concentration on Δ^{14}C is included in the calculations when a varying carbon cycle is assumed. Important for the calculation is the

choice of the starting parameters. The initial amount of ^{14}C in the different reservoirs has an effect on the modelled $\Delta^{14}C$ for several ^{14}C half-lives after the beginning of the calculation. Our calculation starts at 50'000 yr BP with the present ^{14}C inventory and distribution as suggested by the data of Voelcker et al. [27].

The distinction between random and systematic errors is crucial for the calculation of the errors of the modelled $\Delta^{14}C$. To a large extent random errors cancel out since a short-term scatter in the production rate is strongly dampened due to the exchange between the relatively large carbon reservoirs. Systematic errors potentially do not cancel and produce a large band of uncertainty. The dominant systematic errors were included in our calculation. Monte Carlo simulations show that the random errors cause uncertainties of less than $\pm 10‰$ in the modelled $\Delta^{14}C$. This can be neglected compared to the systematic errors.

References

[1] D. Lal, B. Peters, Cosmic ray produced radioactivity on the Earth, in: S. Flügge (Ed.), Handbuch für Physik, Springer, Berlin, 1967, pp. 551–612.

[2] J. Masarik, J. Beer, Simulation of particle fluxes and cosmogenic nuclide production in the Earth's atmosphere, J. Geophys. Res. 104 (1999) 12099–12111.

[3] U. Siegenthaler, M. Heimann, H. Oeschger, ^{14}C variations caused by changes in the global carbon cycle, Radiocarbon 22 (1980) 177–191.

[4] P.U. Clark, N.G. Pisias, T.F. Stocker, A.J. Weaver, The role of the thermohaline circulation in abrupt climate change, Nature 415 (2002) 863–869.

[5] C. Laj, C. Kissel, A. Mazaud, E. Michel, R. Muscheler, J. Beer, Geomagnetic field intensity, North Atlantic Deep Water circulation and atmospheric $\Delta^{14}C$ during the last 50 kyr, Earth Planet. Sci. Lett. 200 (2002) 177–190.

[6] G.M. Raisbeck, F. Yiou, M. Fruneau, J.M. Loiseaux, M. Lieuvin, J.C. Ravel, Cosmogenic $^{10}Be/^{7}Be$ as a probe of atmospheric transport processes, Geophys. Res. Lett. 8 (1981) 1015–1018.

[7] J. Beer, U. Siegenthaler, G. Bonani, R.C. Finkel, H. Oeschger, M. Suter, W. Wölfli, Information on past solar activity and geomagnetism from ^{10}Be in the Camp Century ice core, Nature 331 (1988) 675–679.

[8] E. Bard, G.M. Raisbeck, F. Yiou, J. Jouzel, Solar modulation of cosmogenic nuclide production over the last millenium: comparison between ^{14}C and ^{10}Be records, Earth Planet. Sci. Lett. 150 (1997) 453–462.

[9] F. Yiou, G.M. Raisbeck, S. Baumgartner, J. Beer, C. Hammer, S. Johnsen, J. Jouzel, P.W. Kubik, J. Lestringuez, M. Stiévenard, M. Suter, P. Yiou, Beryllium 10 in the Greenland Ice Core Project ice core at Summit, Greenland, J. Geophys. Res. 102 (1997) 26783–26794.

[10] G. Wagner, C. Laj, J. Beer, C. Kissel, R. Muscheler, J. Masarik, H.-A. Synal, Reconstruction of the paleoaccumulation rate of central Greenland during the last 75 kyr using the cosmogenic radionuclides ^{36}Cl and ^{10}Be and geomagnetic field intensity data, Earth Planet. Sci. Lett. 193 (2001) 515–521.

[11] S.J. Johnsen, D. Dahl-Jensen, W. Dansgaard, N. Gundestrup, Greenland palaeotemperatures derived from GRIP bore hole temperature and ice core isotope profiles, Tellus 47 (1995) 624–629.

[12] K.M. Cuffey, G.D. Clow, Temperature, accumulation, and ice sheet elevation in central Greenland through the last deglaciation transition, J. Geophys. Res. 102 (1997) 26383–26396.

[13] G. Wagner, J. Beer, C. Laj, C. Kissel, J. Masarik, R. Muscheler, H.-A. Synal, Chlorine-36 evidence for the Mono Lake event in the Summit GRIP ice core, Earth Planet. Sci. Lett. 181 (2000) 1–6.

[14] G. Wagner, J. Masarik, J. Beer, S. Baumgartner, D. Imboden, P.W. Kubik, H.-A. Synal, M. Suter, Reconstruction of the geomagnetic field between 20 and 60 kyr BP from cosmogenic radionuclides in the GRIP ice core, Nucl. Instrum. Methods B 172 (2000) 597–604.

[15] R.C. Finkel, K. Nishiizumi, Beryllium 10 concentrations in the Greenland ice sheet project 2 ice core from 3–40 ka, J. Geophys. Res. 102 (1997) 26699–26706.

[16] R. Muscheler, J. Beer, G. Wagner, R.C. Finkel, Changes in deep-water formation during the Younger Dryas cold period inferred from a comparison of ^{10}Be and ^{14}C records, Nature 408 (2000) 567–570.

[17] G. Wagner, J. Beer, P.W. Kubik, C. Laj, J. Masarik, W. Mende, R. Muscheler, G.M. Raisbeck, F. Yiou, Presence of the solar de Vries cycle (205 years) during the last ice age, Geophys. Res. Lett. 28 (2001) 303–306.

[18] M. Stuiver, H.A. Polach, Discussion reporting of ^{14}C data, Radiocarbon 19 (1977) 355–363.

[19] M. Stuiver, P.J. Reimer, E. Bard, J.W. Beck, G.S. Burr, K.A. Hughen, B. Kromer, G. McCormac, J. van der Pflicht, M. Spurk, INTCAL98 radiocarbon age calibration, 24,000–0 cal BP, Radiocarbon 40 (1998) 1041–1083.

[20] T. Goslar, M. Arnold, N. Tisnerat-Laborde, J. Czernik, K. Wickowski, Variations of Younger Dryas atmospheric radiocarbon explicable without ocean circulation changes, Nature 403 (2000) 877–880.

[21] K.A. Hughen, J.R. Southon, S.J. Lehmann, J.T. Overpeck, Synchronous radiocarbon and climate shifts during the last deglaciation, Science 290 (2000) 1951–1954.

[22] H. Kitagawa, J. van der Pflicht, Atmospheric radiocarbon calibration beyond 11,900 Cal BP from Lake Suigetsu laminated sediments, Radiocarbon 42 (2000) 369–380.

[23] J.W. Beck, D.A. Richards, R.L. Edwards, B.W. Silverman, P.L. Smart, D.J. Donahue, S. Hererra-Osterheld,

G.S. Burr, L. Calsoyas, A.J.T. Jull, D. Biddulph, Extremely large variations of atmospheric ^{14}C concentration during the last glacial period, Science 292 (2001) 2453–2458.

[24] E. Bard, M. Arnold, B. Hamelin, N. Tisnerat-Laborde, G. Cabioch, Radiocarbon calibration by means of mass spectrometric $^{230}Th/^{234}U$ and ^{14}C ages of corals. An update data base including samples from Barbados, Mururoa and Tahiti, Radiocarbon 40 (1998) 1085–1092.

[25] E. Bard, B. Hamelin, R.G. Fairbanks, A. Zindler, Calibration of the ^{14}C timescale over the past 30,000 years using mass spectrometric U-Th ages from Barbados corals, Nature 345 (1990) 405–410.

[26] A. Schramm, M. Stein, S.L. Goldstein, Calibration of the ^{14}C time scale to >40 ka by ^{234}U-^{230}Th dating of Lake Lisan sediments (last glacial Dead Sea), Earth Planet. Sci. Lett. 175 (2000) 27–40.

[27] A.H.L. Voelker, P.M. Grootes, M.-J. Nadeau, M. Sarnthein, Radiocarbon levels in the Iceland Sea from 25–53 kyr and their link to the Earth's magnetic field intensity, Radiocarbon 42 (2000) 437–452.

[28] A. Indermühle, E. Monnin, B. Stauffer, T.F. Stocker, Atmospheric CO_2 concentration from 60 to 20 kyr BP from Taylor Dome ice core, Antarctica, Geophys. Res. Lett. 27 (2000) 735–738.

[29] U. Siegenthaler, Uptake of excess CO_2 by an outcrop-diffusion model ocean, J. Geophys. Res. 88 (1983) 3599–3608.

[30] D. Lal, Theoretically expected variations in the terrestrial cosmic-ray production rates of isotopes, in: G.C. Castagnoli (Ed.), Solar Terrestrial Relationships and the Earth Environment in the last Millennia, North-Holland, Amsterdam, 1988, pp. 215–233.

[31] W. Dansgaard, S.J. Johnsen, H.B. Clausen, D. Dahl-Jensen, N.S. Gundestrup, C.U. Hammer, C.S. Hvidberg, J.P. Steffensen, A.E. Sveinbjörnsdottir, J. Jouzel, G. Bond, Evidence for general instability of past climate from a 250-kyr ice-core record, Nature 364 (1993) 218–220.

[32] W.S. Broecker, D.M. Peteet, D. Rind, Does the ocean-atmosphere system have more than one stable mode of operation?, Nature 315 (1985) 21–26.

[33] T.F. Stocker, D.G. Wright, Rapid changes in ocean circulation and atmospheric radiocarbon, Paleoceanography 11 (1996) 773–795.

[34] E. Monnin, A. Indermuehle, A. Daellenbach, J. Flueckiger, B. Stauffer, T.F. Stocker, D. Raynaud, J.-M. Barnola, Atmospheric CO_2 concentrations over the last glacial termination, Science 291 (2001) 112–114.

[35] O. Marchal, T.F. Stocker, R. Muscheler, Atmospheric radiocarbon during the Younger Dryas: Production, ventilation, or both?, Earth Planet. Sci. Lett. 185 (2001) 383–395.

[36] G. Delaygue, T.F. Stocker, F. Joos, G.-K. Plattner, Simulation of atmospheric radiocarbon during abrupt oceanic circulation changes: trying to reconcile models and reconstructions, Quat. Sci. Rev. 22 (2003) 1647–1658.

[37] R.L. Rutberg, S.R. Hemming, S.L. Goldstein, Reduced North Atlantic Deep Water flux to the glacial Southern Ocean inferred from neodymium isotope ratios, Nature 405 (2000) 935–938.

[38] C. Wunsch, Determining paleoceanographic circulations, with emphasis on the Last Glacial Maximum, Quat. Sci. Rev. 22 (2003) 371–385.

[39] W.S. Broecker, T.H. Peng, S. Trumbore, G. Bonani, W. Wölfli, The distribution of radiocarbon in the glacial ocean, Global Biogeochem. Cycles 4 (1990) 103–117.

[40] E.L. Sikes, C.R. Samson, T.P. Guilderson, W.R. Howard, Old radiocarbon ages in the southwest Pacific Ocean during the last glacial period and deglaciation, Nature 405 (2000) 555–559.

[41] A.H.L. Voelker, M. Sarnthein, P. Grootes, H. Erlenkeuser, C. Laj, A. Mazaud, M.-J. Nadeau, M. Schleicher, Correlation of marine ^{14}C ages from the nordic seas with the GISP2 isotope record implications for radiocarbon calibration beyond 25 kyr BP, Radiocarbon 40 (1998) 517–534.

[42] J. Beer, R. Muscheler, G. Wagner, C. Laj, C. Kissel, P.W. Kubik, H.-A. Synal, Cosmogenic nuclides during Isotope Stages 2 and 3, Quat. Sci. Rev. 21 (2002) 1129–1139.

[43] Y. Guyodo, J.-P. Valet, Relative variations in geomagnetic intensity from sedimentary records: the past 200,000 years, Earth Planet. Sci. Lett. 143 (1996) 23–36.

[44] M. Frank, Comparison of cosmogenic radionuclide production and geomagnetic field intensity over the last 200 000 years, Phil. Trans. R. Soc. London 358 (2000) 1089–1107.

[45] S. Yang, H. Odah, J. Shaw, Variations in the geomagnetic dipole moment over the last 12000 years, Geophys. J. Int. 140 (2000) 158–162.

[46] M. Christl, C. Strobl, A. Mangini, Beryllium-10 in deep-sea sediments: a tracer for the Earth's magnetic field intensity during the last 200,000 years, Quat. Sci. Rev. 22 (2003) 725–739.

[47] Y.S. Kok, Climatic influence in NRM and ^{10}Be-derived geomagnetic paleointensity data, Earth Planet. Sci. Lett. 166 (1999) 105–119.

[48] R. Muscheler, Nachweis von Änderungen im Kohlenstoffkreislauf durch Vergleich der Radionuklide ^{10}Be, ^{36}Cl und ^{14}C, PhD Thesis, ETH Zürich, 2000, 165 pp.

[49] S.J. Johnsen, H.B. Clausen, W. Dansgaard, N.S. Gundestrup, C.U. Hammer, U. Andersen, K.K. Andersen, C.S. Hvidberg, D. Dahl-Jensen, J.P. Steffensen, H. Shoji, A.E. Sveinbjörnsdottir, J. White, J. Jouzel, D. Fisher, The $\delta^{18}O$ record along the Greenland Ice Core Project deep ice core and the problem of possible Eemian climatic instability, J. Geophys. Res. 102 (1997) 26397–26410.

[50] P.M. Grootes, M. Stuiver, Oxygen 18/16 variability in Greenland snow and ice with 10^{-3} to 10^5-year time resolution, J. Geophys. Res. 102 (1997) 26455–26470.

[51] S. Baumgartner, J. Beer, G. Wagner, P.W. Kubik, M. Suter, G.M. Raisbeck, F. Yiou, ^{10}Be and dust, Nucl. Instrum. Methods B 123 (1997) 296–301.

[52] A. Indermühle, T.F. Stocker, F. Joos, H. Fischer, H.J. Smith, M. Wahlen, B. Deck, D. Mastroianni, J. Tschumi,

T. Blunier, R. Meyer, B. Stauffer, Holocene carbon-cycle dynamics based on CO_2 trapped in ice at Taylor Dome, Antarctica, Nature 398 (1999) 121–126.

[53] H. Kitagawa, J. van der Plicht, Atmospheric radiocarbon calibration to 45,000 yr B.P.: late glacial fluctuations and cosmogenic isotope production, Science 279 (1998) 1187–1189.

[54] J.R. Petit, J. Jouzel, D. Raynaud, N.I. Barkov, J.-M. Barnola, I. Basile, M. Bender, J. Chapppellaz, M. Davis, G. Delaygue, M. Delmotte, V.M. Kotlyakov, M. Legrand, V.Y. Lipenkov, C. Lorius, L. Pépin, C. Ritz, E. Saltzmann, M. Stievenard, Climate and atmospheric history of the past 420,000 years from the Vostok ice core, Antarctica, Nature 399 (1999) 429–436.

[55] T. Blunier, J. Chapellaz, J. Schwander, A. Dällenbach, B. Stauffer, T.F. Stocker, D. Raynaud, J. Jouzel, H.B. Clausen, C.U. Hammer, S.J. Johnsen, Asynchrony of Antarctic and Greenland climate change during the glacial period, Nature 394 (1998) 739–743.